Absolute Proper Motions to B \sim 22.5: V. Detection of Sagittarius Dwarf Spheroidal Debris in the Direction of the Galactic Anticenter

Dana I. Dinescu^{1,3}, Steven R. Majewski^{2,4}, Terrence M. Girard¹, Réne A. Méndez⁵, Allan Sandage⁶, Michael H. Siegel^{2,7}, William E. Kunkel⁸, John P. Subasavage², and Jamie Ostheimer²

Received	_; accepted
100001100	

¹Astronomy Department, Yale University, New Haven, CT 06520-8101 (dana@astro.yale.edu, girard@astro.yale.edu)

²Department of Astronomy, University of Virginia, Charlottesville, VA 22903-0818 (srm4n@virginia.edu)

³Astronomical Institute of The Romanian Academy, Cutitul de Argint 5, RO-75212 Bucharest 28, Romania

⁴David and Lucile Packard Foundation Fellow, Cottrell Scholar of the Research Corporation

⁵European Southern Observatory, Casilla 19001, Santiago 19, Chile

 $^{^6{\}rm The~Observatories}$ of the Carnegie Institution of Washington, 813 Santa Barbara Street, Pasadena, CA 91101

 $^{^7\}mathrm{Space}$ Telescope Science Institute, 3700 San Martin Drive, Baltimore, MD 21218

⁸Las Campanas Observatory, Casilla 601, La Serena, Chile

ABSTRACT

We have detected a population of predominantly blue $(B-V \leq 1.1)$ stars in the direction $l=167^{\circ}, b=-35^{\circ}$ (Kapteyn Selected Area 71) that cannot be accounted for by standard starcount models. Down to $V \sim 20$, the colors and magnitudes of these stars are similar to those of the southern overdensity detected by the Sloan Digital Sky Survey at $l=167^{\circ}, b=-54^{\circ}$, and identified as stripped material from the Sagittarius dwarf spheroidal galaxy. We present absolute proper motions of the stars in SA 71, and we find that the excess blue stars represent a distinct, kinematically cooler component than the Galactic field, and in reasonable agreement with predictions of Sgr disruption models. The density of the excess SA 71 stars at $V \sim 18.8$ and $B-V \leq 1.1$ is within a factor of two of the density of the SDSS-south Sgr stripped material, and of that predicted by the Helmi & White disruption model. Three additional anticenter fields (SA 29, 45 and 118) show very good agreement with standard starcount models.

Subject headings: Galaxy: structure — Galaxy: halo — galaxies: individual (Sagittarius dwarf spheroidal)

1. Introduction

The Sagittarius dwarf galaxy (Sgr) (Ibata, Gilmore & Irwin 1994) has drawn considerable interest as a "living" example of the accretion process supposedly responsible for the creation of the outer Galactic halo. Most early Sgr surveys focused within 10-15° of its core (e.g., Ibata et al. 1997, hereafter I97, Mateo et al. 1998). More recently, Sgr-associated material has been identified farther from its main body (e.g., Majewski etal. 1999, hereafter M99), and it is becoming apparent that Sgr tidal debris may envelop the whole Galaxy roughly along the satellite's orbit. Results from the Sloan Digital Sky Survey (SDSS) in two equatorial strips (Yanny et al. 2000, hereafter Y00; Ivezic et al. 2000, hereafter I00) find RR Lyrae stars, blue horizontal branch (BHB) stars, and/or blue stragglers (BS) in excess of the Galactic population that are most plausibly explained as Sgr material (see Ibata et al. 2001a). Newberg et al. (2002, hereafter N02) confirm the previous SDSS Sgr detections with color-magnitude diagrams (CMDs) showing main sequence turnoff colors (MSTO) consistent with those of Sgr. Similarly, Martinez-Delgado et al. (2001a,b; collectively referred to as M01) report Sgr detections associated with MSTO stars in several regions along the Sgr orbital path. Vivas et al. (2001) confirm the I00 detection of RR Lyrae stars in a ~ 50 kpc distant clump at positive Galactic latitudes, while Dohm-Palmer et al. (2001) and Kundu et al. (2002; K02 hereafter) report giant star concentrations in the inner halo having radial velocities (RVs) and distances in good agreement with wrapped tidal arms predicted from Sgr disruption models. Ibata et al. (2001b) also show that the carbon-star distribution from the Totten & Irwin (1998, hereafter TI98) all-sky survey is highly correlated with the orbital path of Sgr.

Here we present absolute proper motions and B-V color distributions in Kapteyn Selected Area (SA) 71, a Galactic anticenter field located close to the orbital path of Sgr $(l = 167^{\circ}, b = -35^{\circ})$. We find a population of predominantly blue stars $(B-V \le 1.1)$ in

excess of that predicted by standard Galactic starcount models. The proper motions of the excess blue stars show a distinct, kinematically cooler population than the Galactic field. Assuming that the excess blue stars are horizontal branch (HB) stars, we estimate their distance to be ~ 30 kpc, a value consistent with Sgr disruption model predictions (e.g., Johnston 1998, hereafter J98). We also present B-V color distributions for three other anticenter fields (SA 29, 45 and 118). These allow us to refine some of the parameters of the starcount model. These three fields are consistent with each other and agree with the global model predictions. This work is a continuation of the photometric and proper motion study of SA 57 by Majewski (1992) as well as the Mount Wilson Halo Mapping Project (Sandage 1997).

2. The Data

Star catalogs are derived from typically six Mayall 4m prime focus photographic plates (plate scale $18''.60 \text{ mm}^{-1}$) per field: two each in the J (IIIa-J+GG385), F (IIIa-F+GG495) and R (127-04 + RG610) passbands. In this paper we present only the JF photometry data which we transform to the Johnson BV system (see Majewski 1992). The plates were digitized over a $40'.3 \times 40'.3$ area with the University of Virginia's Perkin-Elmer microdensitometer. The detection of objects, derivation of various image parameters and object classification were performed using the FOCAS software package (Valdes 1982, 1993).

Calibration to standard Johnson *BV* magnitudes used Mount Wilson 100-inch (MW) photoelectric photometry (Sandage 1997, 2000) supplemented with: CCD data for SA 71 and 118 obtained with the Swope 1m telescope at Las Campanas Observatory in 2001 and in 1993 respectively, Massey's (1998) SA 45 data, and, for SA 29, CCD photometry from the Mayall 4m and Mosaic camera. From comparisons between the calibrated photographic and standard photoelectric/CCD magnitudes in the Johnson system, we find uncertainties

in the calibrated magnitudes between 0.05 and 0.12, and in B-V between 0.07 and 0.15, for the relevant magnitude range analyzed here.

Object classification relied on the resolution classifier described by Valdes (1982). Inspection of images and derived image parameters for different classes of objects shows reliable classification to $B \sim 21.2$ ($V \sim 20$). All fields are complete in terms of object detection to $B \sim 22.5$, except SA 118, which is complete to $B \sim 21.5$. These "completeness" limits are 1.5 magnitudes above the plate limit. For the deeper plates, stars brighter than V = 17 show varying degrees of saturation, so we analyze only stars within $17 \leq V \leq 20$. A detailed description of the calibration and object classification will be presented elsewhere.

SA71 proper motions were determined from measurement of thirteen photographic plates spanning a 22-year baseline: eleven Mayall 4m plates (of which six are the plates used for the photometry), and two modern Du Pont 2.5m plates with two exposures (short and long) each. The emulsion+filter combination match the blue, visual and red passbands. The seeing varies between 1 to 3 arcsec, with the modern plates typically having better images. The photometric catalogs served as input lists for astrometric scans with the Yale PDS microdensitometer. General procedures for the astrometric reduction are described elsewhere (e.g., Girard et al. 1998, Dinescu et al. 2000). We have made use of the double exposures on the Du Pont plates to model magnitude-dependent systematics, and have corrected for differential color refraction for the appropriate photographic emulsion and hour angle following the prescription in Dinescu et al. (1996). Inspection of galaxy proper motions shows no detectable trends with colors and magnitudes. We obtain a proper-motion uncertainty of 0.8 mas yr⁻¹ per star for $V \leq 19.5$, and ~ 1 mas yr⁻¹ for V < 20.5. The correction to absolute proper motion is based on ~ 500 galaxies, but has an uncertainty of 0.2 mas yr⁻¹ due to poorer centering accuracy of the galaxy images.

3. Results: Color Distributions and Proper Motions

Stellar color distributions are shown in Figure 1. In each panel, the total counts for the data (left numbers in parentheses) and the starcount model (right numbers) are given. The starcount and kinematical model used here includes representations of the thin and thick disks and the halo. Details of the model can be found in Méndez & van Altena (1996, MvA96) and Méndez & Guzmán (1998). The "best-fit" model parameters were determined by eye from comparisons of all four fields in three V-magnitude bins: 17-18, 18-19, and 19-20. We adopt a maximum thin disk scale-height of 300 pc to represent late-type main sequence stars and white dwarfs. The best-fit thick disk local normalization is 6% of the thin disk with a 1000 pc scaleheight, with a 3.0 kpc scalelength for both disks. The halo is an oblate (c/a = 0.8) de Vaucouleurs law spheroid of local normalization 0.13% to the thin disk. The reddening for a given distance is derived from the extinction model presented in Méndez & van Altena (1998), with infinite distance values from the Schlegel, Finkbeiner & Davis (1998, hereafter SFD) maps for the center of each SA field (SA 29, $E_{B-V} = 0.012$; SA 45, $E_{B-V} = 0.054$; SA 71, $E_{B-V} = 0.219$; and SA 118, $E_{B-V} = 0.025$). The model color counts were convolved with the estimated photometric B-V errors. Field SA 45 partly contains the galaxy M33 in the east part of the field. Therefore, we have analyzed the westernmost $18.5 \times 40'$ region of this field, which shows no M33-contamination in the CMD. For field SA71, which has the largest reddening, we have also determined star counts after dereddening star-by-star according to the SFD maps. The comparison with model counts yields similar results to when a single SA71 reddening value is applied.

The SA 29, 45 and 118 data agree well with model predictions in all three magnitude bins (slight residual systematic errors may still exist in the photographic colors). However, SA 71 shows a clear excess of blue stars for 18 < V < 20 compared to model predictions. This excess occurs for $B - V \le 1.1$, and is most prominent in the 18 < V < 19 bin.

In Figure 2, left panels, we show the vector point diagram (VPD) for 17 < V < 20stars in two color groups: $B - V \le 1.1$ (top panels) and B - V > 1.1 (bottom panels). The blue stars show a clump with dispersion $\sim 2~{\rm mas~yr^{-1}}$ and absolute mean proper motion $\mu_l \cos b = 1.4 \pm 0.3$ and $\mu_b = -0.6 \pm 0.3$ mas ${\rm yr}^{-1}$ superimposed on a field population with wider dispersion. The absolute proper-motion uncertainty is given by the proper-motion measuring error for galaxies and the proper-motion dispersion of the excess blue star clump. The red stars show a wide proper motion distribution typical of the Galactic field. Intuitively, blue field stars have a lower dispersion than red ones, because red stars are predominantly (see Figure 1) nearby disk K-M dwarfs, which have larger proper motions, while blue stars are primarily more distant thick disk and halo stars. However, the adjoining plots of $\mu_l \cos b$ (middle panels) and μ_b (right panels) distributions show more complex character. The continuous lines represent the proper motion distributions predicted from the MvA96 Galactic model, which evidently agree reasonably well with the data for the red stars, whereas the blue sample shows an excess population with a lower dispersion than that of the field. We have also obtained preliminary proper motions in SA 29, a field located symetrically to SA 71 across the Galactic plane. The SA29 proper-motion distributions do not show the excess blue star population seen in SA 71.

4. What is the Excess Population?

In Figure 3 we show in Aitoff projection the location of our SA fields, most known detections (filled symbols) and non-detections (open symbols) of Sgr material, and the orbit of Sgr as determined from the ground-based proper-motion measurement of I97 (continuous line). SA 71 is located close to Sgr's orbit, and to a clump of five carbon stars found in the surveys of TI98 and Green $et\ al.\ (1994)$. These five carbon stars belong to two groups: 1) three stars with R magnitudes 15.1, 15.5, and 16.4 and heliocentric RVs of -133, -140,

and -140 km s⁻¹ respectively (highlighted crosses in Fig. 3); 2) two stars with R = 12.6 and 13.0 and RVs of 112 and 43 km s⁻¹ respectively. Except for the faintest carbon star, which is of CH type, all are N type; according to TI98, the N type can be assigned an absolute magnitude $M_R = -3.5$. Using the SFD reddening values for each location of the carbon stars, we obtain that the fainter group resides at distances 35-44 kpc from the Sun. ¿From the SDSS-south survey (Y00, N02), which is close to SA 71 (Fig. 3), the distance to the candidate Sgr HB stars is ~ 28 kpc. The distances of the carbon stars and of the HB stars in SDSS-south match the distances predicted for tidal debris from Sgr at this Galactic location (see e.g., Helmi & White 2001, hereafter HW01; M01). Moreover, the large, negative RVs of three of the carbon stars (the highlighted crosses in Fig. 3) also match the model predictions for a stream from Sgr that consists of material lost at the previous pericenter passage (Sgr is currently at pericenter, see e.g., HW01, Ibata et al. 2001b).

Considering the proximity of SA 71 to directions where Sgr material has been detected, we can plausibly associate the excess blue stars in SA 71 with Sgr material. For 18 < V < 19 the excess stars peak at $B - V \sim 1.0$ ($[B - V]_0 = 0.78$) a color consistent with Sgr's HB/red clump (Bellazzini, Ferraro & Buonanno 1999). ¿From inspection of the SA 71 CMD, we adopt $V \sim 18.8$ as the magnitude of the candidate Sgr HB, corresponding to a heliocentric distance of 29-32 kpc (the distance range derives from the absolute magnitude spread for RR Lyrae stars of metallicities relevant to Sgr). The estimated distance to the candidate Sgr HB is in agreement with those of the carbon stars, the HB stars found in SDSS-south, and model predictions (HW01, M01). The excess population with 19 < V < 20 is bluer than that with 18 < V < 19, and resembles the BS population found in Y00 and N02.

From kinematics of tidal stream material calculated with the semianalytical disruption model developed by J98 for Sgr and the measured orbit by I97, we find the nearest model Sgr stripped material to SA71 is at $l = 174^{\circ}$, $b = -37^{\circ}$. This material belongs

to a trailing stream that emerged during the previous perigalacticon passage (0.75 Gyr ago). The debris is located 26 kpc from the Sun, and has $\mu_l \cos b = 1.47$ mas yr⁻¹, $\mu_b=-1.67~{
m mas~yr^{-1}},~{
m and}~V_{rad}=-134~{
m km~s^{-1}}.$ The vertical lines in the proper-motion distributions of Fig. 2 represent these predicted proper motions (all are presented in the heliocentric rest frame). To understand better the debris motion, we subtract the reflex solar motion from our SA 71 proper-motion measurement, at a distance of 26 kpc. We obtain $(\mu_l \cos b)' = -0.47 \pm 0.30 \text{ mas yr}^{-1}$, and $\mu_b' = -0.35 \pm 0.30 \text{ mas yr}^{-1}$. For the model predictions we obtain $(\mu_l \cos b)' = -0.43 \text{ mas yr}^{-1}$, and $\mu_b' = -1.55 \text{ mas yr}^{-1}$. While there is good agreement in $\mu_l \cos b$, the predicted value of μ_b is larger in absolute value than that measured. This discrepancy may be due to uncertainties in the model predictions stemming from the 0.7 mas yr⁻¹ uncertainty in the proper motion of Sgr (I97), and/or it may be due to undetected systematics in our proper-motion measurement. A full exploration of models with varying initial conditions may help understand this discrepancy, but is beyond the purpose of this letter. Given the almost polar orbit of Sgr (the latitude of the pole is $b=13^{\circ}$, Ibata et al. 2001b), one might want to compare the direction of our measured velocity vector to that estimated from orbit-shape considerations only. However, we caution that, given the small size of the measured proper motion compared to its uncertainty, the direction is rather poorly constrained. A small-size latitudinal motion is quite conceivable because debris in this particular stream reaches its turning point below the Galactic plane at a Galactic location close to that of SA 71 (see e.g., Fig. 3 in Ibata et al. 2001b).

Assuming a 1.7 mas yr⁻¹ lower limit for the proper-motion dispersion (as given by the μ_b distribution of the excess blue stars), and an 0.8 mas yr⁻¹ measurement uncertainty, we obtain a 213 km s⁻¹ intrinsic velocity dispersion of the clump of blue stars at 30 kpc. This dispersion is too large for a coherent structure to last for 0.75 Gyr. It is more plausible that we sample material lost in several previous passages that is located at various distances, and thus has a wide range in kinematics. The existence of multiple, overlapping Sgr streams

is suggested by M99, Dinescu et al. (2000), Dohm-Palmer et al. (2001), and K02. An alternative or additional explanation is that Galactic thick disk stars contaminate our blue sample and thereby inflate the estimated dispersion (see Fig. 2). As shown by K02, radial velocities can help disentangle streams left by previous Sgr passages, (if this interpretation is correct) and also help separate field stars from Sgr candidates.

The largest excess of blue stars is at 18 < V < 19. The difference between the data and the starcount model for stars with $B-V \le 1.1$ is 47 ± 15 , yielding a density of 0.029 ± 0.009 star arcmin⁻². For the SDSS-south detection, N02 estimate a density three times lower than that of SDSS-north. N02 find 500 red clump stars in the SDSS-north along an orbital path of 4.4° . For our 40'.3 field, the SDSS-south density implies 25 red clump stars, or ~ 2 times lower than our determination. HW01 predict a rather high density of Sgr material at $l = 179^{\circ}$, $b = -35^{\circ}$, a location close to SA 71. They derive a density relative to the main body of Sgr of ~ 0.005 number-counts arcdeg⁻². If the main body of Sgr contains 34,000 red HB stars (Ibata, Gilmore and Irwin [1995] find 17,000 red clump stars within the half-mass radius of the main body of Sgr), then we should find 77 red HB stars in our SA71 area, according to the HW01 model. This number is also within a factor of 2 of our excess counts.

In the future, we plan to supplement this analysis with deeper, more accurate photometry, radial velocities and with detailed modeling of the dynamical evolution of Sgr.

We thank M. Catelan for providing us HB models, M. Irwin for making available the carbon star data, and A. Helmi and K. Johnston for discussions concerning the Sgr disruption models. SRM thanks the Carnegie Observatories for access to Las Campanas facilities. This research was supported by the NSF under grant AST 97-02521.

REFERENCES

- Bellazzini, M., Ferraro, F. R., & Buonanno, R. 1999, MNRAS, 304, 633 Fusi Pecci, F., & Galleti, S. 2001a, AJ, 122, 3171
- Dinescu, D. I., Girard, T. M., van Altena, W. F., Yang, T. -g., & Lee, Y. -W. 1996, AJ, 111, 1205
- Dinescu, D. I., Majewski, S. R., Girard, T. M., & Cudworth, K. M. 2000, AJ, 120, 1892
- Dohm-Palmer, R. C., Helmi, A., Morrison, H., Mateo, M., Olszewski, E. W., Harding, P., Freeman, K. C., Norris, J., & Shectman, S. A. 2001, ApJ, 555, L37,
- Girard, T. M., Platais, I., Kozhurina-Platais, V., van Altena, W. F., & López, C. E. 1998, AJ, 115, 855
- Green, P. J., Margon, B., Anderson, S. F., & Cook, K. H. 1994, ApJ, 434, 319
- Helmi, A., & White, S. D. M. 2001, MNRAS, 323, 529 (HW01)
- Ibata, R., Gilmore, G., & Irwin, M. J. 1994, Nat, 370, 194
- Ibata, R., Gilmore, G., & Irwin, M. J. 1995, MNRAS, 277, 781
- Ibata, R., Wyse, R. F. G., Gilmore, G., Irwin, M. J., & Suntzeff, N. B. 1997 AJ, 113, 634 (I97)
- Ibata, R., Irwin, M., Lewis, G. F., & Stolte, A. 2001a, ApJ, 547, 133
- Ibata, R., Lewis, G. F., Irwin, M., Totten, E., & Quinn, T. 2001b, ApJ, 551, 294
- Ivezic, Z., et al. 2000 AJ, 120, 963 (I00)
- Johnston, K. V. 1998, ApJ, 495, 297 (J98)
- Kundu, A., et al. 2002, ApJ, submitted (K02).
- Majewski, S. R. M. 1992, ApJS, 78, 76

Majewski, S. R., Siegel, M. H., Kunkel, W. E., Reid, I. N., Johnston, K. V., Thompson, I.
 B., Landolt, A. U., & Palma, C. 1999, AJ, 118, 1709 (M99)

Martínez-Delgado, D., Aparicio, A., Gómez-Flechoso, M. A. & Carrera, R., 2001a, ApJ, 549, L199 (M01)

Martínez-Delgado, D., Gómez-Flechoso, M. A., & Aparicio, A. 2001b, in ASP Conf. Ser.,
Observed HR Diagrams and Stellar Evolution, ed. T. Lejeune & J. Fernandes (M01)

Massey, P. 1998, ApJ, 501, 153

Mateo, M., Olszewski, E. W. & Morrison, H. L. 1998, ApJ, 505, L55

Méndez, R. A., & van Altena, W. F. 1996, AJ, 112, 655

Méndez, R. A., & van Altena, W. F. 1998, A&AS, 330, 910

Méndez, R. A., & Guzmán, R. 1998, A&AS, 333, 106

Newberg, H. J., et al. 2002, ApJ, 569, 245 (N02)

Sandage, A. 1997, PASP, 109, 1197

Sandage, A. 2001, PASP, 113, 267

Schlegel, D. J., Finkbeiner, D. P., & Davis, M. 1998, ApJ, 500, 525

Totten, E. J. & Irwin, M. J. 1998, MNRAS, 294, 1

Valdes, F. 1982, in Instrumentation in Astronomy IV, S.P.I.E. Proceedings, Vol. 331

Valdes, F. 1993, FOCAS User's Guide, NOAO document (ftp://iraf/noao.edu/iraf/docs/focas/focasguide.ps.Z)

Vivas, A. K., et al. 2001, ApJ, 554, L33

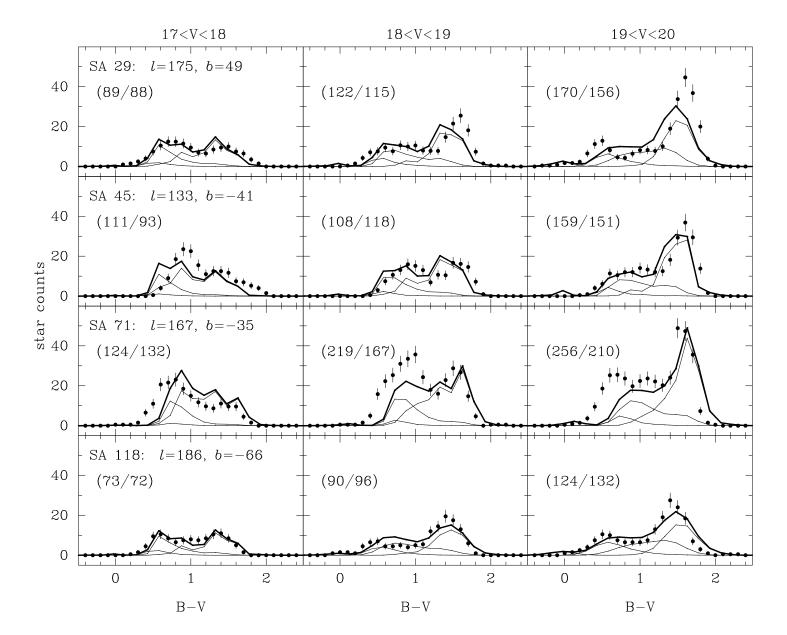
Yanny, B., et al. 2000, ApJ, 540 825 (Y00)

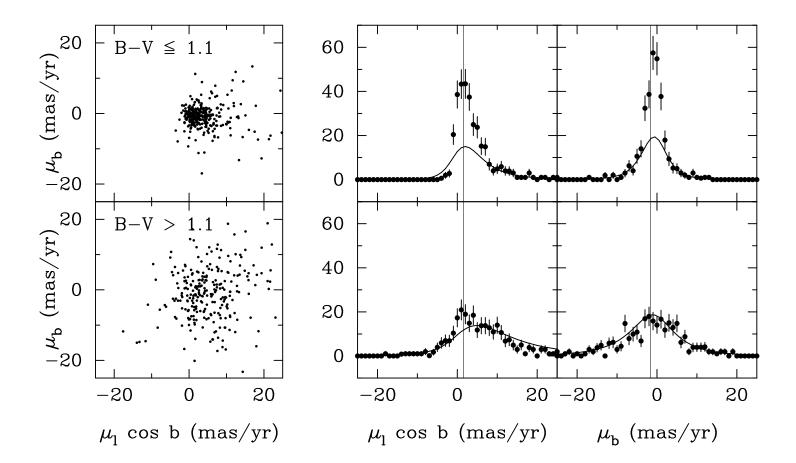
This manuscript was prepared with the AAS LATEX macros v4.0.

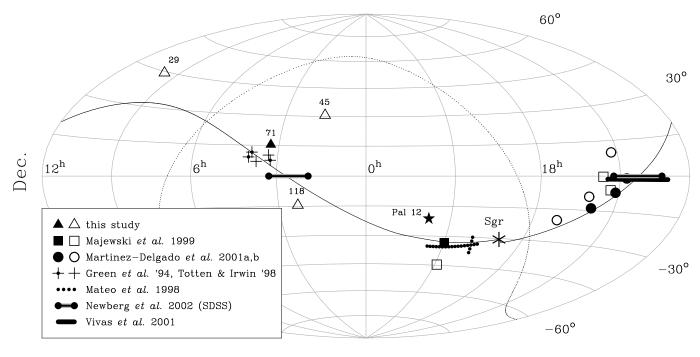
Fig. 1.— B-V color distributions for SA 29, 45, 71 and 118 compared to model predictions. The total model distribution is represented with the thick line. The star counts of each Galactic component are also shown with thin lines. The thin disk dominates the star counts, with smaller contributions from the thick disk and halo. The numbers in each parenthesis represent the data/model counts.

Fig. 2.— VPD (left panels) of stars between V = 17 - 20, and separated into two groups: blue $(B - V \le 1.1;$ top panels) and red (B - V > 1.1; bottom panels). The middle and right panels show the proper-motion distributions in $\mu_l \cos b$ and μ_b respectively compared to model predictions. The vertical lines represent the predicted proper motion of a trailing tidal stream as calculated with the J98 disruption model (see text).

Fig. 3.— Aitoff projection of current detections (filled symbols) and associated non-detections (open symbols) of Sgr material. The projected orbit is represented with a continuous line. The dotted line represents the Galactic plane. Symbols are explained in the legend.







R.A.